Journal of
Water & Climate Change

IWA PUBLISHING

Journal of Water and Climate Change Vol 13 No 9, 3323 doi: 10.2166/wcc.2022.226

Comparative study on stream flow prediction using the GMNN and wavelet-based GMNN

Shivam Agarwal *, Parthajit Roy, Parthasarathi Choudhury and Nilotpal Debbarma

Department of Civil Engineering, National Institute of Technology Silchar, NIT Road, Silchar, Assam 788010, India
*Corresponding author. E-mail: shivamgupta.agarwal@gmail.com

SA, 0000-0001-7221-1171

ABSTRACT

Flood flow forecasting is essential for mitigating damage in flood-prone areas all over the world. Advanced actions and methodology to optimize peak flow criteria can be adopted based on forecasted discharge information. This paper applied the models of the integrated wavelet, multilayer perceptron (MLP), time-delay neural network (TDNN), and gamma memory neural network (GMNN) to predict hourly river-level fluctuations, including storage rate change variable. Accordingly, the researchers initially used the discrete wavelet transform to decompose the water discharge time-series into low- and high-frequency components. After that, each component was separately predicted by using the MLP, TDNN, and GMNN models. The performance of the proposed models, namely wavelet–MLP, wavelet–TDNN, and wavelet–GMNN, was compared with that of single MLP, TDNN, and GMNN models. This analysis affirms that precision is better in the case of integrated models for forecasting river reach levels in the study region. Furthermore, multiple inputs–multiple outputs (MIMO) networks (MIMO-1 artificial neural network (ANN) and MIMO-2 ANN), along with multiple inputs–single output (MISO) ANN were employed for obtaining flow forecasts for several sections in a river basin. Model performances were also evaluated using the root mean squared error having less than 10% of the average mean value, with the coefficient of correlation being more than 0.91 and with the peak flow criteria showing the chances of flash floods being low to moderate with values not more than 0.15.

Key words: artificial neural network (ANN), gamma memory, multiple inputs–multiple outputs (MIMO), river systems, time-delay neural network (TDNN)

HIGHLIGHTS

- The wavelet-based ANN model incorporating storage changes has been accounted for in river flow studies.
- The study is unique while showcasing comparative analysis between different ANNs modeling.
- Flood prediction using pre-processing technique wavelet along with the ANN seems the best model.
- The flood damage mitigation is the need of the hour, which is the main aim for areas prone to heavy precipitation.
- Results seem to be promising.

GRAPHICAL ABSTRACT

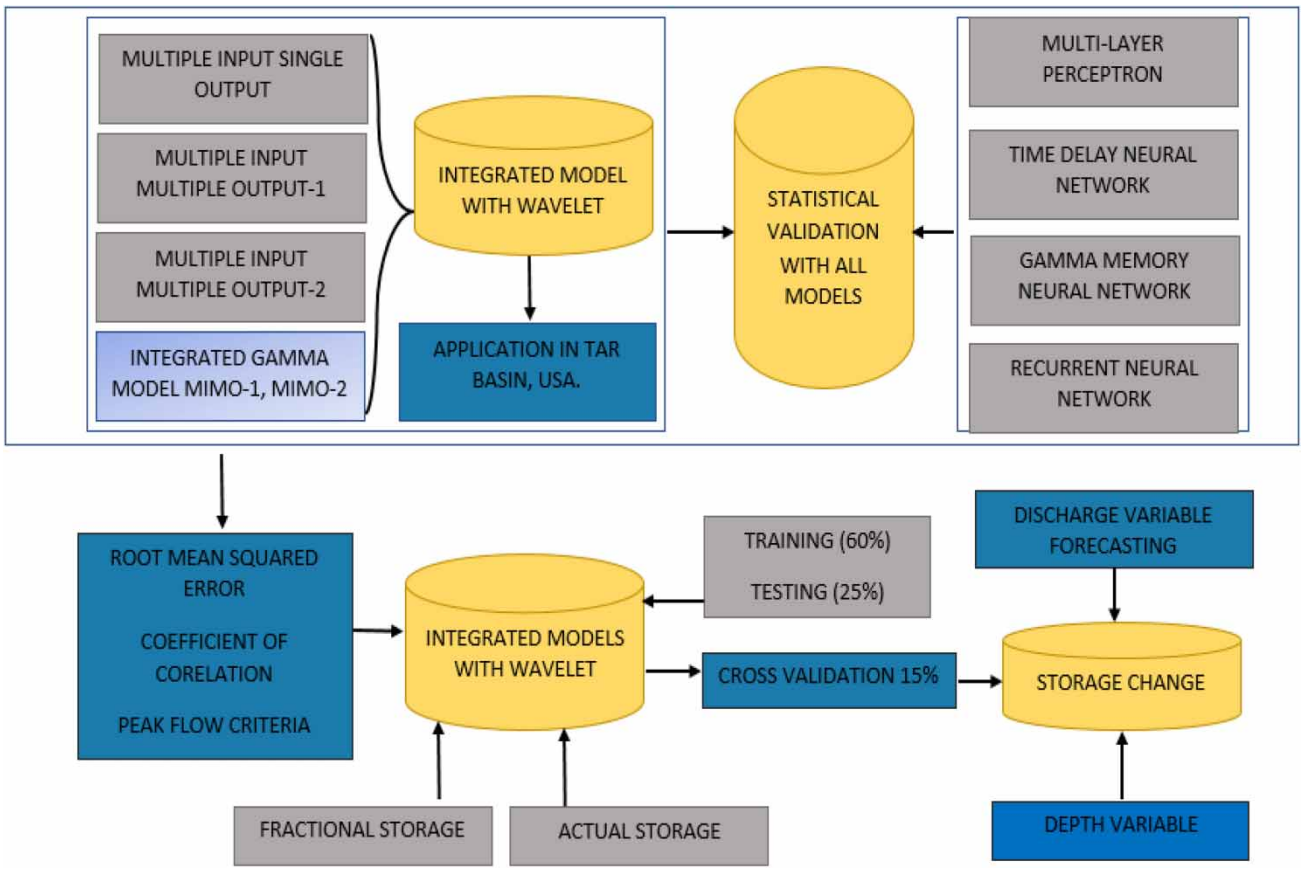

LIST OF ACRONYMS

$Q^{u,p}_{t+\Delta t}$	discharge at an upstream section at time $t+\Delta t$ in a river system
$Q^{d}_{t+\Delta t}$	discharge at downstream section at time $t+\Delta t$ in a river system
$Y^{u,p}_{t+\Delta t}$	flow depth at an upstream section at time $t+\Delta t$ in a river system
$Y^{d}_{t+\Delta t}$	flow depth at downstream section at time $t+\Delta t$ in a river system
y^{u}_{t}, y^{d}_{t}	upstream and downstream flow depth at time t
$Q^{u,e,r}_{t}$	equivalent inflow at a point r in the basin for N upstream flows
c_1, c_3	muskingum routing coefficients
α, β	upstream hydrograph evolution parameters
$Q^{(*)}_{(t)}$	discharge through a river section
ω	parameters for computing discharge from the depth
$y^{(*)}_{(t)}$	depth of flow at a section
$y^{u}_{t+\Delta t}$, $y^{d}_{t+\Delta t}$	upstream and downstream flow depth at time $t+\Delta t$
ω_u, ω_d, η^d, η^u	parameters for computing discharge from depth at upstream
$g_r(t)$	kernel function
$(\mu)^p$	memory resolution
p	memory order

INTRODUCTION

A hydrological forecast represents the preliminary assessments of future hydrological events and their characteristics. Hydrological forecasts are necessary for effective water management and to mitigate the effects of natural hazards, such as floods

and droughts. The prediction of flow in a water system is required to minimize the impact of uncertainties of the climate on the management of water resources, considered one of the main challenges related to integrated knowledge of climatology and hydrology. The use of expected flows for the optimization of river flow operation is suggested by many authors such as Owuor & Mwiturubani (2022) and Beker & Kansal (2022).

Currently, many hydrological models are being used in flood forecasting studies, distributed models or concentrated, conceptual or empirical, discrete or continuous. The objective of studying most of these models is the basis of the simplicity they offer in applying the water balance and mass balance principle. One of the models of the artificial neural network (ANN), the time-delay neural network (TDNN), has been chosen from various models for being an empirical model which has been widely accepted as potentially useful for modeling complex nonlinear systems with a large amount of data. A TDNN can well approximate a number of functional relationships describing outputs that are some functions of the same inputs. These models are especially helpful when it is unclear how the functional link between the input and output data works. The multiple gamma memory neural network (MGMNN) models can also be used in place of and in conjunction with mathematical models.

With this in context, channel inundation, being a multiplex process, is distinguished by spatial and time-related alteration in flow constraints. Applications can be seen in the literature regarding flood flow modeling having the use of the ANN. In most of the ANN models, a multilayer perceptron (MLP) is employed to predict flow variations and storage change except for models deploying the use of time lag feed-forward delays such as the TDNN. Memory in the ANN is assimilating mostly in delays having both feed-forward and feedback. The MLP cannot identify time-related modifications in input series, which is why MLP with a sliding window approach, equivalent to a TDNN, is being implicated in the modeling of temporal variations. Self-recurrent network by Lang *et al.* (1990) can also be an instance of feedback delays in which the input holds the state of past and neural states. Memory depth remains static in the case of the TDNN while training since it cannot scale the time axis. An adaptive ANN can be best suited to find the robust memory depth for which the MGMNN can be best employed.

In an unsteady flow channel, storage and flow rates change concurrently with respect to time. Thus, it may be said that during unsteady flow along with flow rate, flow depths, storage and storage characteristics in reach evolve in time. Hence, a river flow model must also be applicable to river systems with a number of upstream flows and a common downstream flow. Flood flow modeling, being spatially and temporally dependent, requires effective investigation in quantifying the relationship between the use of flood susceptibility maps and the applied machine learning model, since the use of different ANN models on different watershed basins produces results that are dependent on the topographical and geomorphological structures of the river basins (Avand *et al.* 2022).

In 2015, Choudhury and Roy predicted multiple rate flow in river systems using the ANN. The model is based on a time-based application useful in real-time forecasting as flood predictions are time constraints. It is known that during unsteady flow in river reaches, flow rate as well as storage in the channel change continuously with time and are governed by the same causes. Such changes are dependent on common causes such as river reach, watershed basin characteristics and properties, and hydrological and geomorphological properties. Storage change also indicates unsteady flow; therefore, any model utilized for predicting unsteady flow must incorporate storage characteristics. Considering this as a novelty, this study has considered flow rates implicitly as well as explicitly incorporating storage properties. Since storage is as important as flow, therefore, the model meant for predicting unsteady flow must incorporate storage characteristics also. Different storage indicators have been taken to develop a model based on flows and storage characteristics, which is the novelty of this work. In this work, extension and modification of multiple inputs–multiple outputs (MIMO)-based and multiple inputs–single output (MISO)-based model (Aboutalebi *et al.* 2016) have been utilized for using different storage characteristics of which one may be the storage based on the instantaneous storage rate change and the other is the storage based on the gauge height when calculated from an arbitrary datum of the Tar River in North Carolina.

The principle of continuity plays a vital role and has tremendous significance when it comes to river flow modeling. Routing ANN does not incorporate the latter while modeling and training the network architecture. In this study, the basic fundamental continuity principle has been incorporated in order to predict the storage, rate of change of storage, and flow depth variation, which implies the average rate of change in storage properties in the case of MIMO–ANN models. The models in this study obey the continuity equation in the case of MIMO-1 and MIMO-2. But the MISO model does not follow the continuity equation since the weights in the output node are set to zero for all the river sections, excluding the forecasting section. The result shows that all ANNs very accurately matched the pre-decided zero value at the sections.

River flow forecasting is an essential aspect of flood damage mitigation and plays a vital role in water resource management. The characteristics of river flow are governed by various factors and results of different factors, such as precipitation, evapotranspiration, and groundwater discharge (Ardiclioglu *et al.* 2022). Recently, various artificial intelligence techniques, such as MLP, TDNN, gamma memory, and adaptive neuro-fuzzy inference system (ANFIS), have been employed for forecasting hydrological phenomena, which are highly nonlinear in nature and are continuously changing with time (Choudhury & Roy 2015). The MLP has the potential to match flow parameters almost with full precision but does not comply with continuity equation norms in the mass balance of river flow.

Since the last decade, artificial intelligence has promised many advantages in data feeding in computers directly without any simplification, and it has been utilized in various applications in hydrology (Kerh & Lee 2006). Kerh & Lee (2006) projected and forecasted the river flow for flood using the information at upstream stations, and Karunanithi *et al.* (1994) predicted the streamflow using an ANN model. The authors also found that ANNs have better performance in comparison with an analytic nonlinear power model. Furthermore, Tayfur & Guldal (2006) employed ANN models for monthly streamflow forecasting and observed that neural network methods perform better than statistical methods. Tingsanchali & Keokhumcheng (2006) also discussed the ANN-based literature to forecast river flows ranging from 1 day to 1 year in the River of Thailand using only past flow observations.

Mostly, ANN-based flow models in river flow studies purposely comply with matching input–output sequences to forecast the flow, as in the case of the study of Kerh & Lee (2006), where they used a routing-type ANN in river outreaches. Routing-type ANN models should observe continuity norms to satisfy the mass balance in a river reach/river system. Nonetheless, the routing-type ANN models that are available in the literature do not consider storage variation and, hence, may not fully satisfy the law of conservation of mass in river reaches while issuing a forecast. ANN models for river flow studies commonly employ static MLPs to predict the flow variables. Maier & Dandy (2000) reviewed 43 studies that dealt with the prediction and forecasting of water resource-related variables and reported that all but only two studies used static MLP networks. Moreover, flood flow in river reaches is highly nonlinear and time-varying and is characterized by changes in channel storage and flow rates at bounding sections over time (Thirumalaiah & Deo 1998). An MLP is a feed-forward and static network with no recursion or memory elements; mapping in the MLP being instantaneous, it cannot recognize and integrate temporal variations in input sequences (Giles *et al.* 1997). Thus, the applications of the static MLP in forecasting flood flows, which is a time-varying process, may not be preferable if the accuracy and timeliness of forecasts must be catered to. Shukla *et al.* (2022) studied that depth–discharge forecasting requires actual field data and has a significant effect on model performances. They also emphasized the use of the actual length of training data by using multi-artificial intelligence models. They found that an ANFIS gives better results than simple ANN models. They also formulated depth–discharge relations by using various ANN techniques coupled with wavelet.

Given that the state of a time-dependent process is a function of its previous states, ANN models that can store and utilize past information are found to be more efficient in analyzing these processes. Broadly, memory by feed-forward delays and memory by feedback delays classify ways to incorporate short-term memory in the neural network system. Lang *et al.* (1990) classified memory by feed-forward delays as a TDNN, which involves the explicit inclusion of delays in the neural network system. In the case of memory by feedback delays, recurrent units hold a trace of the past input and self-recurrent network of Elman & Zipser (1988) and Jordan (1986). Static MLP-type ANN models with a sliding window approach, which are equivalent to a TDNN, have been utilized in modeling temporal variations (Jain *et al.* 1999; Tokar & Johnson 1999; Coulibaly *et al.* 2000a, 2000b). In this case, a fixed number of past information selected by the user is presented as inputs to the MLP network.

As fixed numbers of past samples are used as inputs, the network possesses a fixed or static memory. Most of the ANN-based flood forecasting models available in the literature are capable of providing forecasts at a single location and do not possess forecast updating capability (Agarwal *et al.* 2021b). This restricts the applicability of these models in real-time situations (Coulibaly *et al.* 2001). A TDNN creates memory by delaying the input sequences, and its application in river flow studies is available in the work of Coulibaly *et al.* (2000b). A limitation of TDNN and MLP with memory is that with memory depth being fixed and pre-decided, the selected memory depth does not match the temporal characteristics of river flow studies, thereby giving poor results. Hence, transforming a river reach on a large scale and specifying calculating characteristics for river flow even with a small catchment now depend on the geomorphological river reach characteristics (Varentsova *et al.* 2020). Singh *et al.* (2021) categorized the flood plain into critical zones and developed it by considering topographical aspects. Therefore, topography also plays a critical role in flood flow modeling. On the basis of the literature

study, the following broad objectives are attempted in the present study: to formulate an ANN-based flow forecasting model for a river system incorporating storage characteristics, and to evaluate the performances of different memory-based ANN models along with the use of wavelet technique in forecasting flows incorporating storage variations in river reaches.

MODELS AND METHODS

Concurrent storage predicting models with MIMO forms

A MIMO-1 ANN has $(n+1)$ output nodes of which the rth nodes provide the real flow forecast for the rth bounding section while the remaining nodes are fixed to zero-rate flow as forecasts for other sections.

It may be emphasized here that this formulation has a significant advantage in real-time forecasting as alongside forecasting the flow variable, the level of forecasting accuracy achieved can be judged by considering the errors made in matching the known flow rate and flow depth values for other stations.

$$Q^{u,p}_{t+\Delta t} = f^n(Q^{u,1}_t, Q^{u,2}_t, Q^{u,3}_t, \ldots, Q^{u,N}_t\ ;\ Q^d_t, \psi, \phi);\quad \forall\, p;\quad p = 1, 2, 3, \ldots, N \tag{1}$$

$$Q^d_{t+\Delta t} = g(Q^{u,1}_t, Q^{u,2}_t, Q^{u,3}_t, \ldots, Q^{u,p}_t, \ldots, Q^{u,N}_t\ ;\ Q^d_t, \psi, \phi) \tag{2}$$

The MISO models rely on matching flow usually at one downstream section only using a number of upstream flows. Equations (1) and (2) describe the fractional-storage change in the MIMO model form having different functional values on each input. Fractional-storage change in MIMO-1 form combined together may depict the actual storage variation since MIMO-1 models are complementary to each other and sum together, depicting actual storage change.

In the case of the MISO ANN, as the input–output data arrangements conform neither to the actual flow variation nor to the storage variation in the reach, the inclusion of storage characteristics in mapping the forecasted flow is of least significance. Applying flow depth variables for boundary channel flow in a catchment, Equations (3) and (4) can be obtained as given in Equations (1) and (2).

$$Y^{u,p}_{t+\Delta t} = G^n(y^{u,1}_t, y^{u,2}_t, y^{u,3}_t, \ldots, y^{u,N}_t\ ;\ y^d_t, \psi', \phi');\quad \forall\, p;\quad p = 1, 2, 3, \ldots, N \tag{3}$$

$$Y^d_{t+\Delta t} = H^n(y^{u,1}_t, y^{u,2}_t, y^{u,3}_t, \ldots, y^{u,N}_t\ ;\ y^d_t, \psi', \phi'); \tag{4}$$

MISO ANNs do not comply with storage rate consideration in river flow since it only provides output with one single node, i.e., forecasting station while feeding various multiple inflows section, as it does not follow the principle of continuity, hence of least importance.

$$Q^{u,e,r}_t = \sum_{p=1}^{n} \sigma^{p,r} Q^p_t \tag{5}$$

$$Q^{u,e,r}_{t+\Delta t} = \frac{1}{-(1 - c_1 - c_3)}(c_1 \alpha Q^{u,e,r}_t + c_3 \beta Q^d_t) \tag{6}$$

$$Q^d_{t+\Delta t} = c_1(1 - \alpha)Q^{u,e,r}_t + c_3(1 - \beta)Q^d_t \tag{7}$$

where c_1 and c_3 stand for the Muskingum model parameters, whereas α and β are upstream hydrograph evolution parameters. Equivalent flow is split into two complementary parts for upstream and downstream flows having storage, $\alpha Q^{u,e,r}_t \rightarrow Q^{u,e,r}_{t+\Delta t}$ and $\beta Q^d_t \rightarrow 0$ in Equation (6) and $(1 - \alpha)Q^{u,e,r}_t \rightarrow 0$, $(1 - \beta)Q^d_t \rightarrow Q^d_{t+\Delta t}$ in Equation (7).

It may be mentioned that the MIMO-1 models, when trained using flow variables, only implicitly learn storage change characteristics for the reach during a period. To make the networks learn the storage variation characteristics explicitly from the data set rate of storage change data computed using instantaneous inflow and outflow rates and instantaneous average flow depth data computed using known concurrent flow depths at the bounding sections in the reach may be used along with the flow rate/flow depth data in training the network.

Based on the literature survey, Agarwal *et al.* (2021a) computed storage rate change implicitly. With this in context, storage rate change has been computed explicitly in this work, satisfying the continuity norm. MIMO-1 is mapping all outputs to zero except for the forecasting sections. MIMO-1 ANN, learns characteristic fractional-storage changes providing a forecast for flow variables at a single section only.

Multiple input multiple output-2

As the MIMO-1 is mapping all outputs to zero except for the forecasting sections, two MIMO-1 networks mapping upstream and downstream future flow, respectively, for a single reach may be summed, obtaining a single MIMO-2 network that has the same (two) inputs as the MIMO-1 network and two outputs representing real flow forecast for the upstream and downstream sections, respectively.

It is evident that a MIMO-2 network explicitly learns flow variations in the upstream and downstream sections, and as indicated by the continuity principle, the networks also implicitly learn the actual storage variation in the reach during the period. It may be pointed out that a MIMO-2 network learns actual storage variation, whereas a MIMO-1 learns a fractional-storage variation such that $(N+1)$ fractional-storage variations learned by the MIMO-1 ANNs always sum to the actual variation learned by the MIMO-2 network.

In the case of a river system having $(N+1)$ flow series, all the series can be forecasted by training a single MIMO-2 network with concurrent $(N+1)$ inputs and concurrent $(N+1)$ outputs separated by a time interval Δt.

Relationship between discharge and depth of flow

The relationship between discharge $Q_{(t)}^{(*)}$ passing through a river section and the depth of flow $y_{(t)}^{(*)}$ at the sections is usually described by a power relation given as the following:

$$Q_{(t)}^{(*)} = \omega (y_{(t)}^{(*)})^{\eta} \tag{8}$$

Equations (2), (5), and (6) reformulate the models using depth variables (Agarwal *et al.* 2021a). That is, by employing Equation (8) in conjunction with Equations (5) and (6), the 'end of the period' flow depth for the upstream and downstream stations can be written as a function (Choudhury 2007; Choudhury & Sankarasubramanian 2009) of the current flow depths at the upstream and downstream stations as given in Equations (9) and (10).

$$y_{t+\Delta t}^{u} = \left\{ \frac{1}{-(1-c_1-c_2)\omega_u} (c_1 \alpha \omega_u (y_t^u)^{\eta^u}) + c_3 \beta \omega_d (y_t^d)^{\eta^d} \right\}^{\frac{1}{\eta^u}} \tag{9}$$

$$y_{t+\Delta t}^{d} = \left\{ \frac{1}{\omega_d} (c_1 (1-\alpha) \omega_u (y_t^u)^{\eta^u}) + c_3 (1-\beta) \omega_d (y_t^d)^{\eta^d} \right\}^{\frac{1}{\eta^d}} \tag{10}$$

Multiple gamma memory neural network

The MGMNN is an extended version of an MLP having dynamic memory parameters that are self-adaptable and adjustable based on input pattern sequences. Having feedback connections that are restrained by local units, it is in the form of a recurrent neural network having both feedback and feed-forward connections and memory structures. Since the adjustable memory adapts and adjusts itself perfectly to the best possible memory depth while training, it has the advantage over other memory-based ANNs models for a pattern that recognizes temporal variation in input sequences. Memory in gamma of P order is a single input–multi-output linear structure where the impulse response in the regular time of the pth tap is given by (Coulibaly *et al.* 2000b; Choudhury & Ullah 2014)

$$g_r(t) = \frac{(\mu)^p}{(p-1)!} t^{p-1} e^{-\mu t}; \quad p = 1, 2, 3 \ldots . P(\mu > 0) \tag{11}$$

Here, μ is a memory parameter representing memory resolution. The generating kernels $g_r(t)$ are the integrands of the gamma function ($\Gamma(\mathrm{x}) \equiv \int_0^{\alpha} t^{\mathrm{x}-1} e^{-t} \mathrm{d}t$), and thus the memory is called the gamma memory.

The gamma memory has an adjustable memory parameter μ that can be optimized during the training period selecting the best possible memory depth for a time-varying pattern. In the case of a focused MGMNN model, a number of gamma memories, one at each node in the input layer, are used, and, thus, the model can process multiple time-varying inputs using different memory depths as in Shukla *et al.* (2022). In this study, the applicability of gamma neural networks having adaptive memory has been investigated since gamma memory incorporates both feedback and feed-forward memory parameters, and while training, it can adjust its memory resolution for a time-varying pattern. The MGMNN possesses an adaptive memory to select the best duration in the past that the network should remember for giving the best result.

In the case of a river system having N upstream flows, Equations (5) and (6) can be written using equivalent inflow as follows (Choudhury & Sankarasubramanian 2009; Choudhury & Ullah 2014; Choudhury & Roy 2015):

$$Q_{t+\Delta t}^{u,e,r} = \frac{1}{-(1-c_1-c_3)}(c_1\alpha Q_t^{u,e,r} + c_3\beta Q_t^d), \tag{12a}$$

$$Q_{t+\Delta t}^{d} = c_1(1-\alpha)Q_t^{u,e,r} + c_3(1-\beta)Q_t^d, \tag{12b}$$

$$Q_t^{u,e,r} = \sum_{p=1}^{N} \sigma^{p,r} Q_t^p. \tag{12c}$$

where $Q_t^{u,e,r}$ is the equivalent inflow at point r in the basin for N upstream flows measured at various locations; and $\sigma^{p,r}$ is the shift factor associated with the transfer of flow from p to r. Given the above fractional-storage variations for a river system, each upstream flow and the common downstream flow at time $\boldsymbol{t}+\Delta\boldsymbol{t}$ can be written explicitly as functions of flow rates at time t for all sections in the system as given in Equations (13a) and (13b) (Choudhury & Sankarasubramanian 2009; Choudhury & Roy 2015).

$$Q_{t+\Delta t}^{u,p} = f^n(Q_t^{u,1}, Q_t^{u,2}, Q_t^{u,3}, \ldots, Q_t^{u,N};\ Q_t^d, \psi, \phi); \quad \forall p; \quad p = 1, 2, 3, \ldots, N. \tag{13a}$$

$$Q_{t+\Delta t}^{d} = g(Q_t^{u,1}, Q_t^{u,2}, Q_t^{u,3}, \ldots, Q_t^{u,p}, \ldots, Q_t^{u,N};\ Q_t^d, \psi, \phi) \tag{13b}$$

With the application of the flow depth variables for the bounding sections in a river system, Equations (13a) and (13b) can be obtained as given in Equations (13c) and (13d) (Choudhury 2007; Choudhury & Roy 2015).

$$y_{t+\Delta t}^{u,p} = g^n(y_t^{u,1}, y_t^{u,2}, y_t^{u,3}, \ldots, y_t^{u,N};\ y_t^d, \psi', \phi'); \quad \forall p; \quad p = 1, 2, 3, \ldots, N \tag{13c}$$

$$y_{t+\Delta t}^{d} = G(y_t^{u,1}, y_t^{u,2}, y_t^{u,3}, \ldots, y_t^{u,p}, \ldots, y_t^{u,N};\ y_t^d, \psi', \phi') \tag{13d}$$

Most of the flood forecasting models were developed using discharge and/or depth variables only. Although during the flood flow, storage in river reaches continuously changes along with the bounding section flow rates, these storage variables are required to be included in the model to accurately compute desired flow rates and the damages caused. In the present study, different categories of the model using the artificial intelligence technique and incorporating storage change-related variables have been developed and applied for real-life river system flood flow analysis (Equations (13a)–(13d)).

Studies have been conducted to capture variation in one variable at a time and also to capture variation in all the variables simultaneously (Equations (12a) and (12c)). Both the models agree with the continuity equation. The application of the widely used MISO model that does not explicitly agree with the continuity equation has been covered in the study.

Wavelet neural network based on gamma memory

A wavelet neural network (WNN) transform is a new signal analysis and processing technology that has emerged in the past one or two decades. WNN is a new type of feed-forward network combining wavelet theory and ANN. In forward transmission, the input signal is processed layer by layer from the input layer through the hidden layer to the output layer, and the error is backpropagated. Unlike Back Propagation (BP) neural networks, in WNNs, the wavelet basis function is used instead of the Sigmoid function as the excitation function.

The reduction and translation variables make WNNs have both the characteristics of the time–frequency localization of the wavelet transform and the self-learning characteristics of the neural network, and the network has a strong approximation ability and also improves generalization (Choudhury & Roy 2015).

The Sigmoid function equation is as follows:

$$F(x) = \frac{1}{(1 + e^{-ax})}, \tag{14}$$

where 'a' is the incentive value.

When modeling natural systems such as floods, the problem of noisiness and nonlinearity of real data often occurs. This problem is partly solved with the help of such filtration. Data filtering always arises when it is necessary to separate the signal from the noise that distorts it. Here, the signal is ordered as a set of numerical information about the process, i.e., time-series; the signal source can be any change ratio system. The purpose of data filtering is to restore change of the original signal against the background of interference or the definition of a proper signal and, therefore, the reduction of data unreliability. There are many filtering methods, and many of them can be applied in the creation of information systems of analysis and forecasting, but the one of wavelet is considered the most promising transformation. One of the urgent tasks of digital processing signals is cleaning the signal from noise.

Since any real signal contains not only useful information but also interference, this model can be written as:

$$S(t) = f(t) + k*e(t), \tag{15}$$

where $S(t)$ is the signal under study; $f(t)$ is a useful signal; k is the noise level; and $e(t)$ is the noise.

The task of filtering is to maximize the possible reduction of the second term in (15). Filtering a signal using wavelet transformations is performed in the following four stages:

- The decomposition of the signal in terms of the wavelet basis.
- The choice of the noise threshold value for each decomposition level.
- The threshold filtering of detail coefficients.
- Signal recovery.

For the wavelet transform, two indicators are critical: the order of the wavelet and the depth of decomposition. Wavelet depth–an indicator that determines the smoothed sharpness–the higher this value, the smoother the reconstructed signal. It should be noted that smoother wavelets create a smoother signal approximation and vice versa (wavelets with a small depth of the peaks of the approximated functions). The depth of decomposition determines the scale of shifted parts: the more significant this value, the larger signal changes will be discarded, i.e., the depth of decomposition can be called the degree of signal chopping.

Wavelet analysis employs standard wavelets. The fact that wavelets are spatially localized is their most significant advantage. Data compression, data processing, and the solution of differential equations all use these algorithms.

STUDY AREA AND DATA DESCRIPTION

In the present study, a network of the river system and a single river reach in the Tar-Pamlico River basin located in North Carolina, USA, have been selected for estimating and forecasting the river flow rates at all the bounding sections of river systems/reach. The model forms MIMO-1, MIMO-2, and MISO have been selected for modeling river flows in the Tar-Pamlico River basin, North Carolina, USA, employing the ANN models, namely MLP-I, TDNN, and MGMNN. A brief description of the study area and data are presented in Figure 1, where the application of the models for forecasting river flows at the gauging sites of the selected river systems of river basins is made by using past recorded data for the basins.

Past recorded concurrent flow information for five gauging sites–Rocky Mount, Hilliardston, Enfield, Tarboro, and Greenville–is used in the present study to forecast flow at each of the gauging sites. Concurrent flow records for the gauging sites of the basin starting from 29 July 2004 to 20 October 2004 with an interval of 15 min were collected from the United States Geological Survey (USGS) instantaneous streamflow Data Archive (http://ida.water.usgs.gov/ida/available_records.cfm). Instantaneous streamflow values are continuous streamflow values recorded at intervals of 15 min and are converted into 2-h intervals.

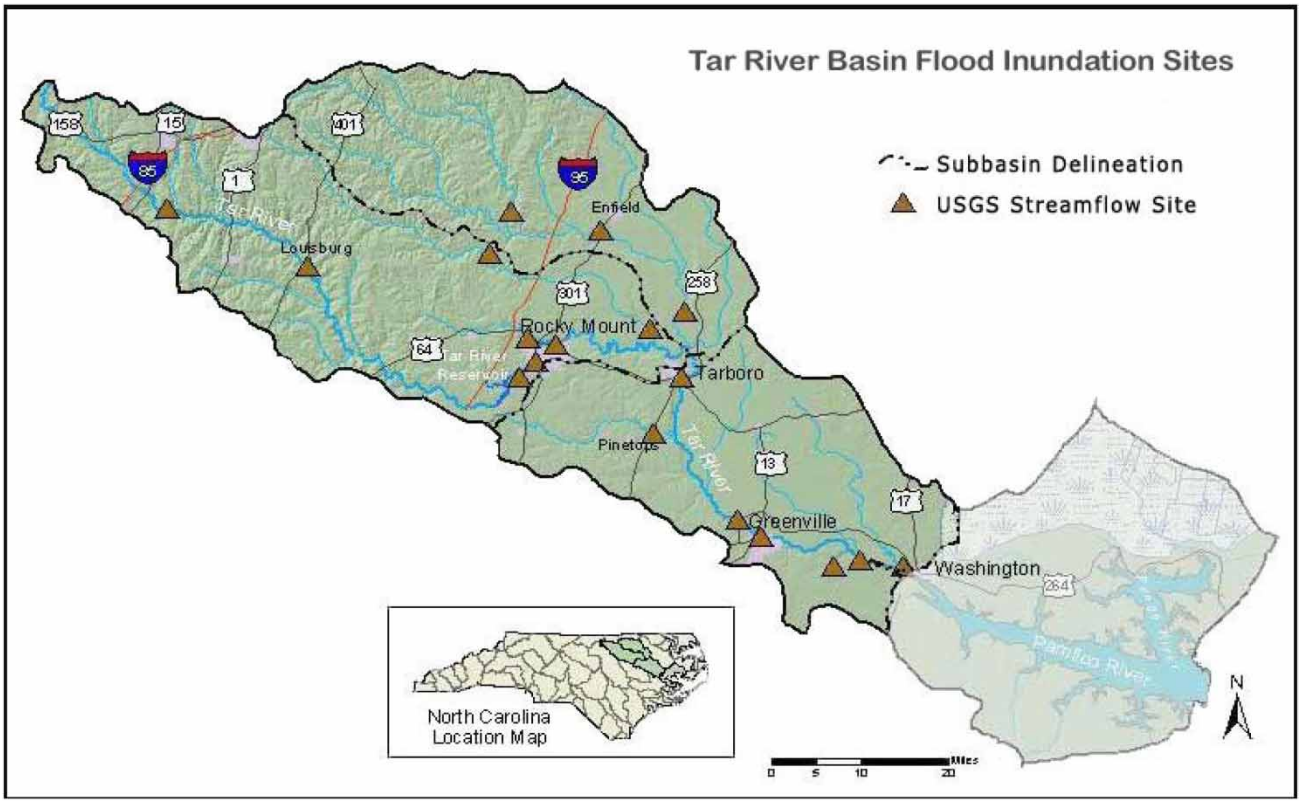

Figure 1 | The map of all the gauging stations in the Tar River Basin of the study area.

RESULTS AND DISCUSSION

In the present study, ANN having no memory, i.e., multilayer perceptron MLP and having memory (i.e., TDNN and gamma memory) are utilized to develop flood forecasting models. The models use water level and discharge as inputs. Input–output data sets collected for five stations in the Tar River system are used to forecast downstream flood flows. In the Tar River Basin, three stations, namely Enfield, Hilliardston, and Rocky Mount, are considered upstream stations, and the remaining two stations (i.e., Greenville and Tarboro) are considered downstream stations. Furthermore, MISO and MIMO forecasting models predict the flood while considering common downstream outflow features depending upon the topography and river basin characteristics. The present study depicts the flow forecast while considering storage rate change, an important criterion for river flow modeling satisfying the principle of continuity. Table 1 depicts the model's performances in terms of root mean squared error (RMSE) and various other statistical criteria incorporating storage rate changes explicitly. Additionally, in Figure 2 'dsdt', which is instantaneous storage rate change, and 'delta S', representing average storage, can

Table 1 | Model performances based on various statistical criteria in MIMO-2, including storage rate change

Model	Performance	Inflow (Upper Tar River Basin)		Outflow (Lower Tar River Basin)	
Gamma memory neural network (**MGMNN**)		**MIMO-2 actual storage rate change**	**MIMO-1 fractional-storage rate change**	**MIMO-2 actual storage rate change**	**MIMO-1 fractional-storage rate change**
	RMSE	305	280	295	298
	CE	0.91	0.95	0.93	0.98
	R	0.98	0.96	0.91	0.94

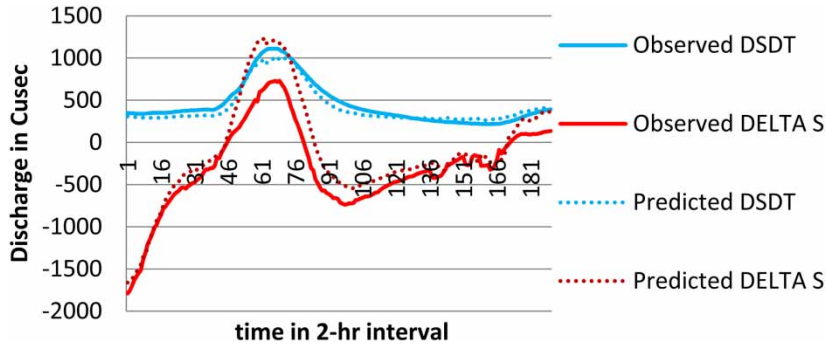

Figure 2 | Observed and one-time-step ahead forecasted instantaneous storage rate and delta S flow at Tarboro (starting from 00:00 h of 29 July) using a wavelet–MIMO-1 MGNN Model.

be seen in observed and forecasted state using the wavelet MIMO-1 MGNN model. The model formulation is mainly focused on the study of characteristics of fractional and actual variations of storage during the unsteady flow of rivers. The applicability of models is evaluated using performance criteria like the coefficient of correlation and many other statistical criteria. Results depict that the ANN having an adaptable memory depth for gamma memory is best suited for real-time flood forecasting considering the storage rate change. In this model, the value of the coefficient of correlation is approximately 0.98, which indicates its satisfactory performance. Furthermore, the maximum RMSE is approximately 20% less than the corresponding observed mean. The study demonstrates the applicability of the ANN for flood forecasting, considering the storage rate change that follows the principle of continuity.

The performances are presented in Table 1 for the MIMO-2 model form vs. MIMO-1 model form when validated. Here, the RMSE error comes around less than 10% of the observed mean value, which is a positive sign for validation as shown in Figure 3, where the MIMO-1 model forms with respect to the MIMO-2 model in terms of discharge in cusec for various inflow and outflow stations, except for the case of an outflow station where discharge value is much higher for inflow stations. Figure 4 illustrates the prediction of time-series data with the predicted flow rates having 2 h of lead time. The results shown

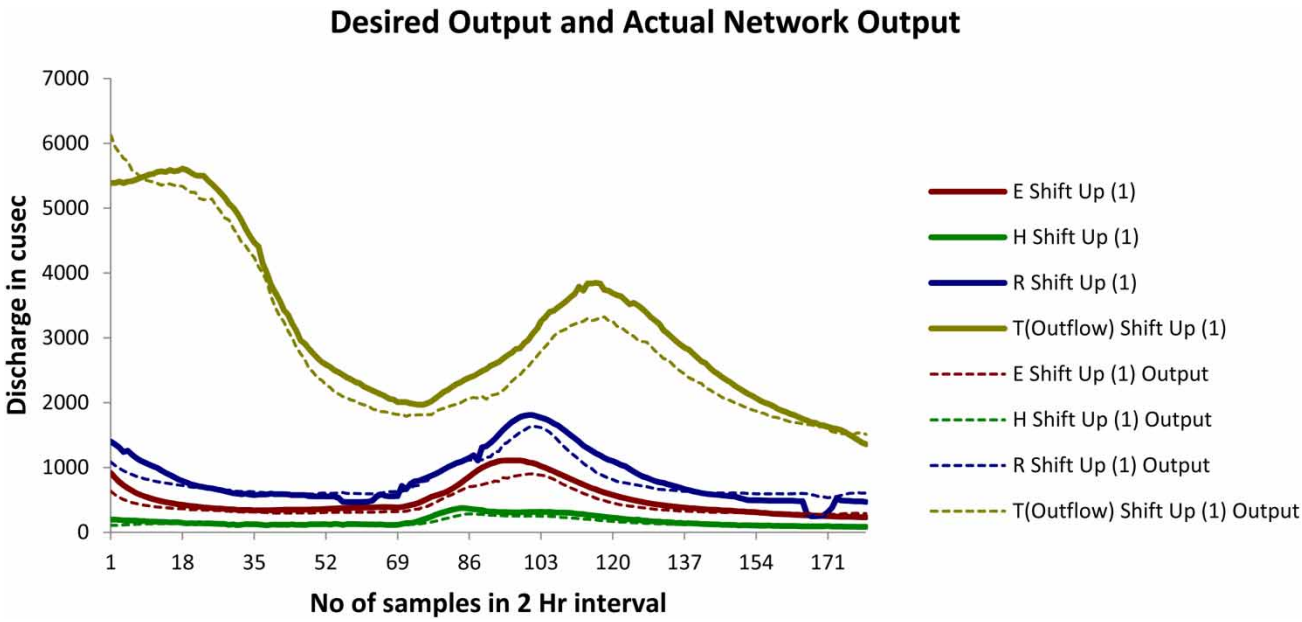

Figure 3 | An implicit validation of the MIMO-1 model form with respect to the MIMO-2 model in terms of discharge in cusec for various inflow and outflow stations.

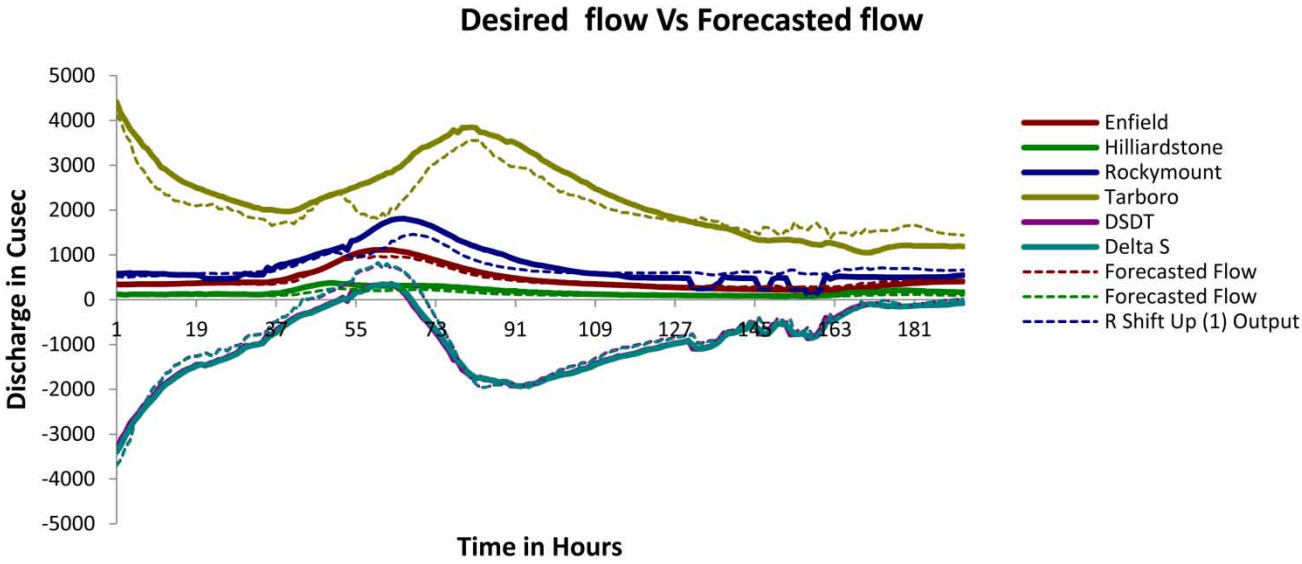

Figure 4 | Desired and 2-h ahead predicted flows for various sections in the Tar River Basin obtained by using an integrated wavelet MIMO-2 MGMNN.

here are of testing data sets, 25% of the entire input set. Here, the discharge is in cusec on the *Y*-axis and time in a 2-h gap interval on the *X*-axis. The study area, which is the catchment of the Tar River Basin, USA, is shown in Figure 1. Gauging stations, Enfield, Rocky Mount, and Hilliardston, are taken as inflow stations, whereas Greenville is considered a downstream gauging station. Table 2 shows the major outcome for the prediction of flash flood occurrences in the basin area using various ANN architectures. It can be inferred from values calculated in Table 2 that flash flood variations prevailing for August, September, and October 2004 are minimal in nature. Hence, the chances of river flow flooding are much less during that period. Storage rate change implies instantaneous storage calculation while considering inflows stations, i.e., Enfield, Hilliardston, and Rocky Mount and the outflow station Tarboro.

In the case of delta S, calculated on the basis of the average storage rate, assuming that initially the storage is zero at the beginning and multiplying the delta S with the time interval gap, the total amount of water can be obtained.

The calculation of PFC for all the bounding stations is conducted by the formula given subsequently, where $Q_t^{o,r}$ denotes discharge at an observed location at time t and $Q_t^{f,r}$ represents discharge at a forecasted station at time t. Table 2 shows the model performances in terms of peak flow criterion when it comes to forecasting flow rate using the MIMO-1 model

Table 2 | Model performances in terms of PFC for forecasting flow rates by using the MIMO-1 form of ANN models in the Tar Basin

Forecasting stations	Models	DSDT (storage rate change)	Delta storage
Enfield	Gamma	0.0913	0.1366
	MLP	0.1061	0.0916
	TDNN	0.1058	0.1650
Rocky Mount	TDNN	0.1254	0.1556
	Gamma	0.1292	0.1556
	MLP	0.0898	0.1335
Tarboro	Gamma	0.1080	0.0864
	MLP	0.0515	0.0517
	TDNN	0.1087	0.1090
Hillardston	Gamma	0.1669	0.1304
	MLP	0.1232	0.1021
	TDNN	0.0987	0.0950

form in the Tar River Basin.

$$PFC = \frac{\left(\sum_{t=1}^{T_p} (Q_t^{o,r} - Q_t^{f,r})(Q_t^{o,r})^2\right)^{\frac{1}{4}}}{\left(\sum_{t=1}^{T_p} (Q_t^{o,r})^2\right)^{\frac{1}{2}}} \tag{16a}$$

These values imply that there is a moderate-to-very low chance of occurrence of flood during the stipulated time interval. Since the storage values calculated do not show much variation for the given time in Peak Flow Criteria (PFC) calculation. Tables 3 and 4 exhibit the value of RMSE, coefficient of efficiency (CE), and coefficient of correlation (R) before and after wavelet decomposition. The results verify that there is little improvement in these values updated due to the pre-processing of the input data set. Wavelet has removed noise from the input data set, thereby making it more precise to obtain feed-forward from ANNs. Tables 3 and 4 forecast and validate various statistical criteria in the MIMO-1 and MIMO-2 forms, whereas Tables 5 and 6 show that the values obtained from statistical criteria showcase the differences in value in inflow and outflow stations, respectively. Enfield, Hilliardston, and Rocky Mount are considered various upstream flows, whereas Tarboro is regarded as an outflow station.

Weights and parameters are assigned to the optimized WNN, and from July to October 2004, forecast samples were applied. In addition, the daily hourly flow from July to October 2004 was predicted. The prediction results are compared with the WNN and BP network prediction values. The forecast test uses three methods, namely MISO, MIMO-1, and MIMO-2. Tables 5 and 6 show the comparative results, and it can be observed that the prediction result of the WNN is better than that of the simple MLP network and that after the gamma algorithm optimization (Liu *et al.* 2021), the prediction accuracy has greatly been enhanced. In the wavelet model optimized by the gamma algorithm, in July, August, and September 2004, the reported value was almost consistent with the actual measured value, and the relative error was less than the results obtained in the simple MLP which achieved a very accurate forecast accuracy. The dotted lines show forecasted flow discharge, and the regular lines in the graph predict the observed or desired flow discharge in feet cube per second.

Table 3 | Performances of MGMNN ANN models in forecasting storage change rate changes in the Tar River Basin before wavelet decomposition

Performance	Enfield	Hilliardston	Rocky Mount	Tarboro	DSDT (rate change storage)	Delta storage
RMSE	63.38	66.08	217.12	393.99	211.73	209.41
NMSE	0.06	0.63	0.28	0.20	0.07	0.07
MAE	52.83	53.84	172.95	341.69	171.16	169.29
Min abs error	0.06	1.53	1.50	0.66	1.54	0.79
Max abs error	167.18	146.56	572.23	983.92	543.57	503.69
R	0.98	0.96	0.92	0.94	0.98	0.98

Table 4 | Performances of MGMNN ANN models in forecasting storage change rate changes in the Tar River Basin after wavelet decomposition

Model	Performance	Inflow (Upper Tar River Basin)		Outflow (Lower Tar River Basin)	
Gamma memory neural network (**MGMNN**)		**MIMO-2 actual storage rate change**	**MIMO-1 fractional-storage rate change**	**MIMO-2 actual storage rate change**	**MIMO-1 fractional-storage rate change**
	RMSE	256	265	274	291
	CE	0.91	0.96	0.94	0.98
	R	0.98	0.97	0.95	0.96

Table 5 | Performances of MGMNN ANN models in forecasting flow at time *t* at a section by learning storage rate changes over an interval of the Δt variation along with the flow variation in the Tar River Basin (before wavelet decomposition)

Model	Performance measure	Inflow (Upper Tar River Basin)		Outflow (Lower Tar River Basin)	
Gamma memory neural network (**MGMNN**)		**Enfield**	**Hilliardston**	**Rocky Mount**	**Tarboro**
	RMSE	34.12	18.55	68.21	81.12
	CE	0.99	0.94	0.95	0.98
	R	0.95	0.97	0.91	0.92

Table 6 | Performances of MGMNN ANN models in forecasting flow at time *t* at a section by learning storage rate changes over an interval of the Δt variation along with the flow variation in the Tar River Basin (after wavelet decomposition)

Model	Performance measure	Inflow (Upper Tar River Basin)		Outflow (Lower Tar River Basin)	
Gamma Memory Neural Network **MGMNN**		**Enfield**	**Hilliardston**	**Rocky Mount**	**Tarboro**
	RMSE	31.02	16.12	65.02	80.01
	CE	0.99	0.95	0.96	0.98
	R	0.95	0.98	0.92	0.96

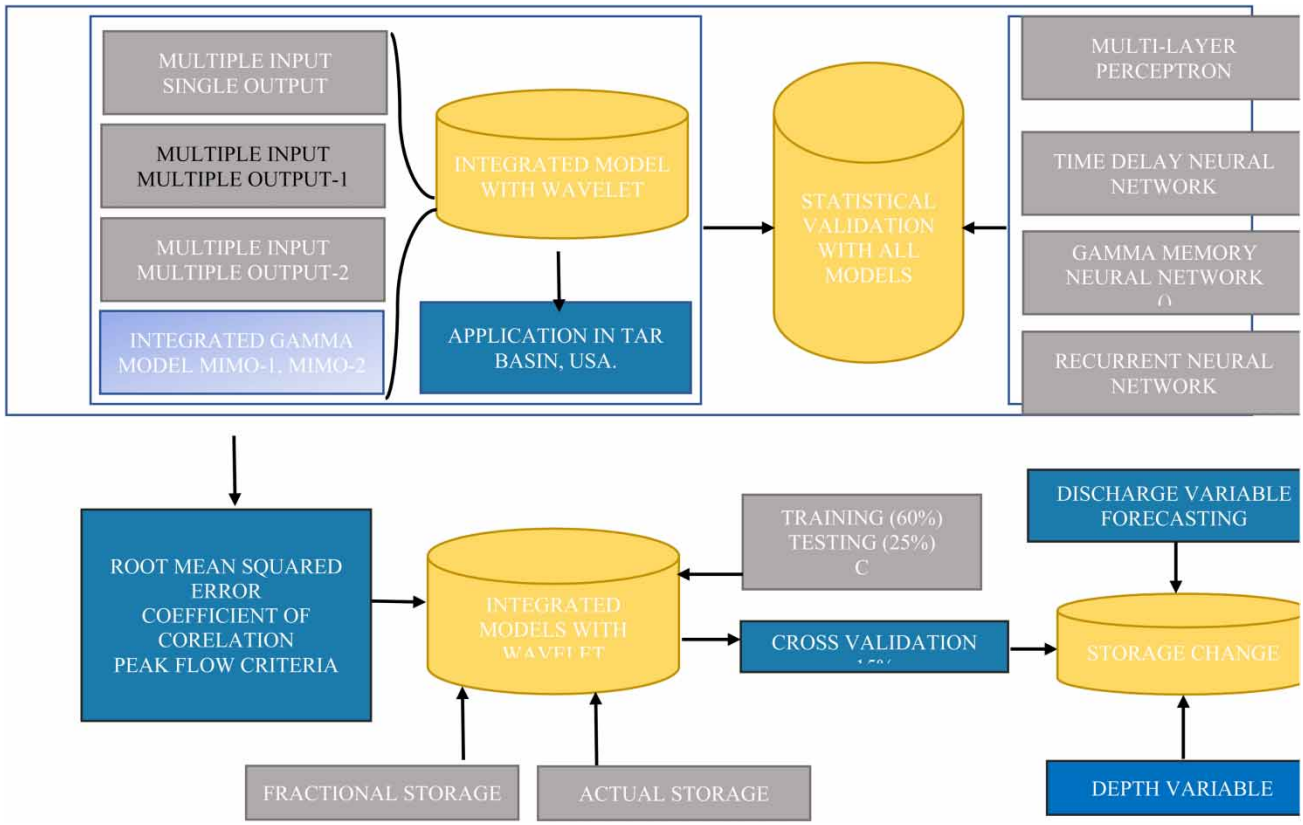

Figure 5 | The flow chart of the modeling process.

CONCLUSION

Daily-based hourly-scale river forecasting has significant seasonality and trend. Choudhury & Roy (2015) developed the model using an ANN in river flow studies using gamma memory and a TDNN, but they did not account for storage. Storage

rate change and storage variables are critical factors that must be accounted for when it comes to river flow modeling. The storage model concept is introduced as a phase of flood disaster management to visualize the picture of forecasts. As the flow forecast is a time-bounded process depending on the evolution of flow parameters such as discharge, depth of flow, and also storage which too is a time-varying variable, incorporation of it is a must to visualize the completeness in river flow forecast. There is a need for an integrated storage model to effectively picture the complete scenario of the flood. In every case of the forecast, it has been found that the storage forecast model, along with discharge and depth, is performing well. In all cases, the results depicted are satisfactory, though, in each and every case, results may not be on a par with and better than previously used models; the incorporation of storage in the prediction of spatial-time-bounding flood is undoubtedly of much importance. This incorporation is justified since it completely visualizes the importance of storage parameters in this time-bounding flood forecasting. Otherwise, it can be a limitation or a drawback in the study. Some variables were left out of the picture, which is equally important, and now this has been included in the MIMO-1 and MIMO-2 models along with all the variables like discharge and the depth of flow. Figure 5 depicts the flow chart of the entire flood flow modeling process. This study uses a neural network with gamma memory along with the storage rate change variable, and the inter-sequence model establishes a forecasting model. The daily hourly flow of the Tar-Pamlico River Basin in North Carolina is forecasted and tested, which has already been conducted in the work of Choudhury & Roy (2015) but without storage. In addition, this paper is an extension of the work performed by Choudhury & Roy (2015) while incorporating storage as a flow variable. In the present study, the applications of ANN models in predicting concurrent flows in the Tar River Basin by using a single and a number of trained networks are presented. ANNs having no memory, static memory, and adaptive memory are used to predict the concurrent flow rate in multiple sections in the Tar River Basin, USA. The model formulations MIMO-1 and MIMO-2 are based on learning storage characteristics fractionally and absolutely during unsteady flows in river reaches. The study shows that to forecast the concurrent flows by using MIMO networks, either a single MIMO-2 or as many MIMO-1 networks as the number of bounding sections in a river system can be trained that can learn storage variation characteristics. The MIMO-1 and MIMO-2 ANNs satisfy continuity requirements for a reach implicitly; the study shows that MIMO-1 and MISO ANNs are different forms of the MIMO-2 ANN obtained by constraining the outputs and connections to the output nodes from the hidden layer to zero–for all sections except the forecasting section in a river reach/system. Pre-processing techniques, such as wavelet, enhance the result to a minimum of 5–10% by removing noise from the input data set.

DATA AVAILABILITY STATEMENT

All relevant data are available from https://waterdata.usgs.gov/nc/nwis/current/?type=flow.

CONFLICT OF INTEREST

The authors declare there is no conflict.

REFERENCES

Aboutalebi, M., Haddad, O. B. & Loáiciga, H. A. 2016 Application of the SVR-NSGAII to hydrograph routing in open channels. *Journal of Irrigation and Drainage Engineering* **142** (3), 04015061.

Agarwal, S., Roy, P. J., Choudhury, P. & Debbarma, N. 2021b Flood forecasting and flood flow modeling in a river system using ANN. *Water Practice and Technology* **16** (4), 1194–1205. https://doi.org/10.2166/wpt.2021.068.

Agarwal, S., Roy, P. J., Choudhury, P. S. & Debbarma, N. 2021a River flow forecasting by comparative analysis of multiple input and multiple output models form using ANN. *H2Open Journal* **4** (1), 413–428. https://doi.org/10.2166/h2oj.2021.122.

Ardiclioglu, M., Hadi, A. M. W. M., Periku, E. & Kuriqi, A. 2022 Experimental and numerical investigation of bridge configuration effect on hydraulic regime. *International Journal of Civil Engineering*. https://doi.org/10.1007/s40999-022-00715-2.

Avand, M., Kuriqi, A., Khazaei, M. & Ghorbanzadeh, O. 2022 DEM resolution effects on machine learning performance for flood probability mapping. *Journal of Hydro-Environment Research* **40**, 1–16. ISSN 1570-6443.

Beker, B. A. & Kansal, M. L. 2022 Fuzzy logic-based integrated performance evaluation of a water distribution network. *Journal of Water Supply: Research and Technology-Aqua* **71** (3), 490–506.

Choudhury, P. 2007 Multiple inflows Muskingum routing model. *Journal of Hydrologic Engineering* **12** (5), 473–481.

Choudhury, P. & Roy, P. 2015 Forecasting concurrent flows in a river system using ANNs. *Journal of Hydrologic Engineering* **20** (8), 06014012.

Choudhury, P. & Sankarasubramanian, A. 2009 River flood forecasting using complementary Muskingum rating equations. *Journal of Hydrologic Engineering* **14** (7), 745–751.

Choudhury, P. & Ullah, N. 2014 Downstream flow top width prediction in a river system. *Water SA* **40** (3), 481–490, 982–994.

Coulibaly, P., Anctil, F. & Bobee, B. 2000a Daily reservoir inflow forecasting using artificial neural networks with stopped training approach. *Journal of Hydrology* **230** (3–4), 244–257.

Coulibaly, P., Anctil, F. & Bobee, B. 2000b Neural network-based long-term hydropower forecasting system. *Computer-Aided Civil and Infrastructure Engineering* **15** (5), 355–364.

Coulibaly, P., Anctil, F. & Bobee, B. 2001 Multivariate reservoir inflow forecasting using temporal neural networks. *Journal of Hydrologic Engineering* **6** (5), 367–376.

Elman, J. L. & Zipser, D. 1988 Discovering the hidden structure of speech. *Journal of the Acoustical Society of America* **83**, 1615–1626.

Giles, C. L., Lawrence, S. & Tosi, A. C. 1997 Rule inference for financial prediction using recurrent neural networks. In *Proc., IEEE/IAFE Conference on Computational Intelligence for Financial Engineering*, IEEE Press, Piscataway, N.J, pp. 253–259.

Jain, S. K., Das, D. & Srivastava, D. K. 1999 Application of ANN for reservoir inflow prediction and operation. *Journal of Water Resources Planning and Management* **125** (5), 263–271. ASCE.

Jordan, M. I. 1986 Attractor dynamics and parallelism in a connectionist sequential machine. In *Proc. 8th Annual Conference of the Cognitive Science Society*, pp. 531–546.

Karunanithi, N., Grenney, W. J., Whitley, D. & Bovee, K. 1994 Neural networks for river flow prediction. *Journal of Computing in Civil Engineering* **8** (2), 201–220. ASCE.

Kerh, T. & Lee, C. S. 2006 Neural networks forecasting of flood discharge at an unmeasured station using river upstream information. *Advances in Engineering Software* **37** (8), 533–543. ISSN 0965-9978. https://doi.org/10.1016/j.advengsoft.2005.11.002.

Lang, K., Waibel, A. H. & Hinton, G. E. 1990 A time-delay neural network architecture for isolated word recognition. *Neural Networks* **3** (1), 23–44.

Liu, X., Sang, X., Chang, J., Zheng, Y. & Han, Y. 2021 Water demand prediction optimization method in Shenzhen based on the zero-sum game model and rolling revisions. *Water Policy* **23** (6), 1506–1529.

Maier, H. & Dandy, G. 2000 Neural networks for the prediction and forecasting of water resources variables: a review of modeling issues and applications. *Environmental Modelling and Software* **15**, 101–124. doi:10.1016/S1364-8152(99)00007-9.

Owuor, M. O. & Mwiturubani, D. A. 2022 Correlation between flooding and settlement planning in Nairobi. *Journal of Water and Climate Change*. **13** (4), 1790–1805.

Shukla, R., Kumar, P., Vishwakarma, D. K., Ali, R., Kumar, R. & Kuriqi, A. 2022 Modeling of stage-discharge using back propagation ANN-, ANFIS-, and WANN-based computing techniques. *Theoretical and Applied Climatology* **147**, 867–889. https://doi.org/10.1007/s00704-021-03863-y.

Singh, R. K., Soni, A., Kumar, S., Pasupuleti, S. & Govind, V. 2021 Zonation of flood prone areas by an integrated framework of a hydrodynamic model and ANN. *Water Supply* **21** (1), 80–97.

Tayfur, G. & Guldal, V. 2006 Artificial neural networks for estimating daily total suspended sediment in natural streams. *Nordic Hydrology* **37**, 69–79.

Thirumalaiah, K. & Deo, M. 1998 River stage forecasting using artificial neural networks, technical papers. *Journal of Hydrologic Engineering* **3** (1). doi:10.1061/(ASCE)1084-0699(1998)3:1(26).

Tingsanchali, T. & Keokhumcheng, Y. 2006 Flood damage functions for surrounding area of Second Bangkok International Airport. In: *Proceedings, International Symposium on Urban Safety of Mega Cities in Asia*, Phuket, Thailand, pp. 291–300.

Tokar, A. S. & Johnson, P. A. 1999 Rainfall runoff modelling using artificial neural networks. *Journal of Hydrologic Engineering* **4** (3), 232–239. ASCE.

Varentsova, N. A., Kireeva, M. B., Frolova, N. L., Kharlamov, M. A., Ilich, V. P. & Sazonov, A. A. 2020 Forecasting water inflow into the Tsimlyansk Reservoir during spring flood under current climate conditions: problems and reproducibility. *Water Resources* **47** (6), 953–967.

First received 18 March 2022; accepted in revised form 12 August 2022. Available online 6 September 2022